Electronic Supplementary Material (ESI) for RSC Advances.

Solution-gel-based surface modification of $LiNi_{0.5}Mn_{1.5}O_{4-\delta}$ with amorphous Li-Ti-O coating

Fulya ULU OKUDUR[1], Maria BATUK[2], Joke HADERMANN[2], Mohammadhosein SAFARI[3], Dries DE SLOOVERE[1], Satish Kumar MYLAVARAPU[1], Bjorn JOOS[1], Jan D'HAEN[4], Marlies K. VAN BAEL[1] and An HARDY[1]

Supporting information

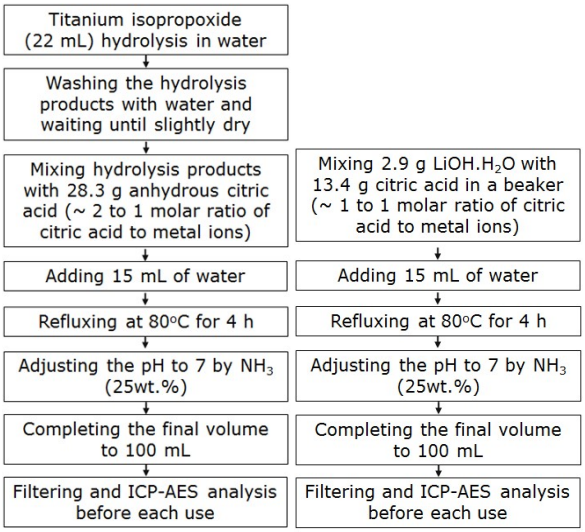

(a) (b)

Figure S1. (a) Titanium (0.4 M) and (b) lithium (0.6 M) precursor solutions synthesis flowcharts

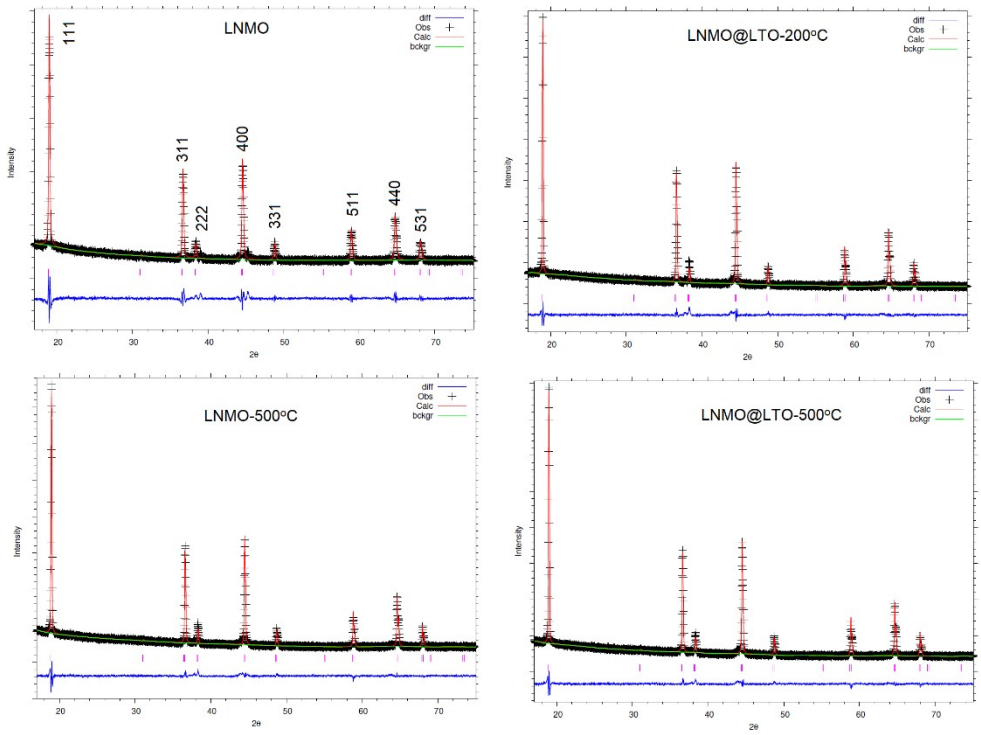

Figure S2. Refinement profiles of bare and LTO surface modified LNMO powders

Table S1. Refinement results obtained from XRD data of LNMO samples

Sample	a (Å)	$\%R_{wp}$	$\%R_{Bragg}$	$\chi 2$
LNMO	8.150556(211)	5.57	8.59	2.751
LNMO@LTO-200ºC	8.162390(106)	3.93	3.47	1.764
LNMO-500ºC	8.163114(103)	3.95	3.27	1.797
LNMO@LTO-500ºC	8.161614(94)	3.82	2.94	1.719

Table S2. Atom sites used for $LiNi_{0.5}Mn_{1.5}O_{4-\delta}$ lattice parameter refinements [1]

atom	site	x	y	z	site occupancy
Li	8a	0.125	0.125	0.125	1
Ni	16d	0.5	0.5	0.5	0.25
Mn	16d	0.5	0.5	0.5	0.75
O	32e	0.26314(6)	0.26323(5)	0.2632(7)	1

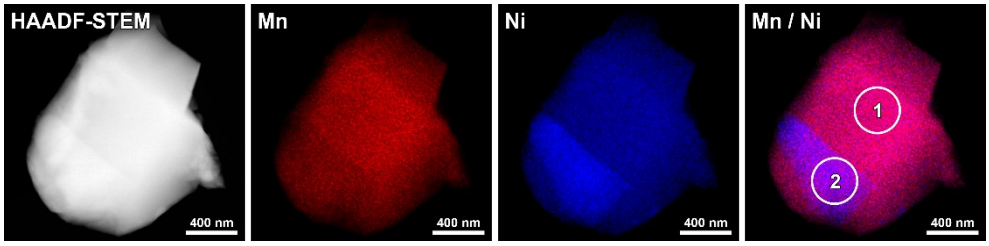

Figure S3. LNMO-500°C: HAADF-STEM image, individual STEM-EDX maps, and Mn/Ni mixed map. The Ni and Mn content in the LNMO crystal when Li and O are neglected (area 1) is 24 and 76 at.% and in the Ni-rich area (area 2) is 45 and 55 at.%, respectively.

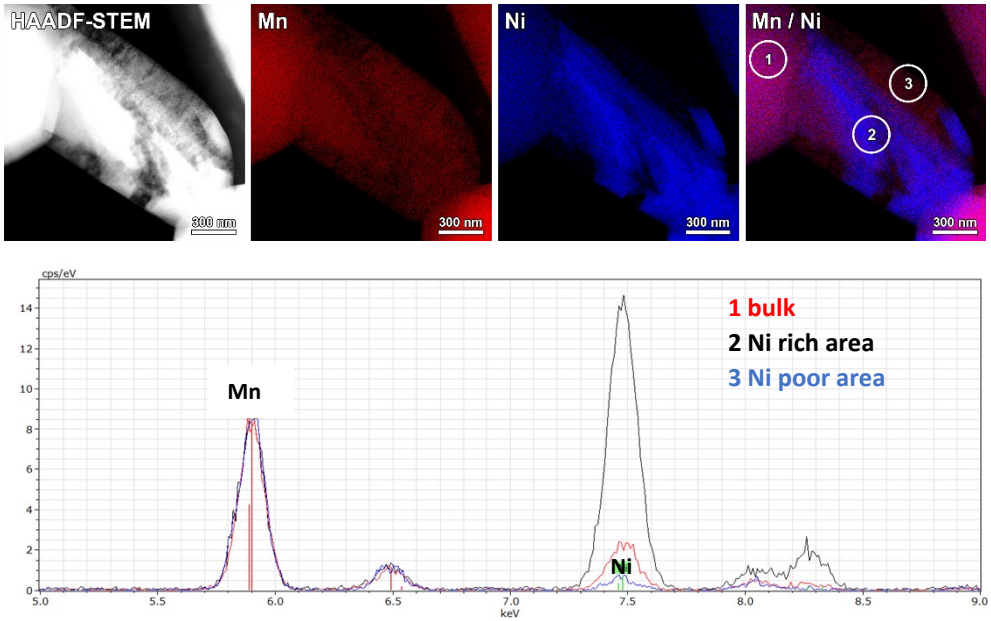

Figure S4. LNMO@LTO-200°C: HAADF-STEM image, individual STEM-EDX maps, and Mn/Ni mixed map from the Ni-rich particle. The EDX spectra measured from areas 1-3 were normalized to Mn content. Crystal (1) is a typical LNMO crystal with Ni to Mn at. ratio 24/76 when Li, Ti and O are neglected. Ni-rich area (2) showed Ni to Mn atomic ratio 68/32. Ni-poor area (3) showed Ni to Mn atomic ratio 8/92.

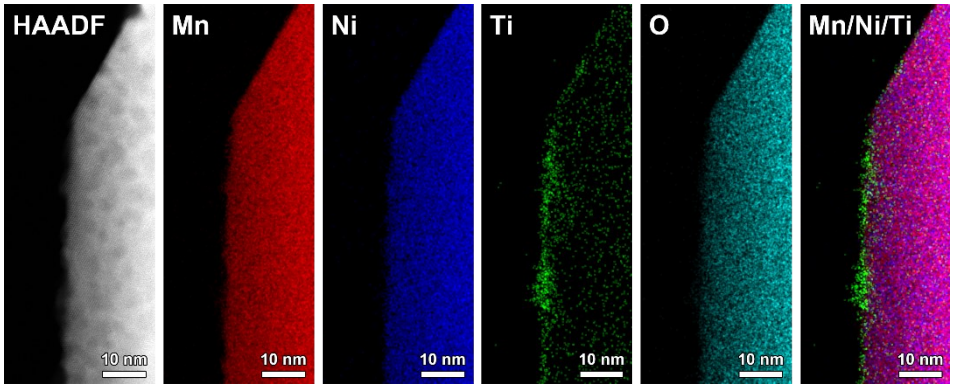

Figure S5. LNMO@LTO-200°C: HAADF-STEM image, individual STEM-EDX maps and Mn/Ni/Ti mixed map from the Ti-coated surface.

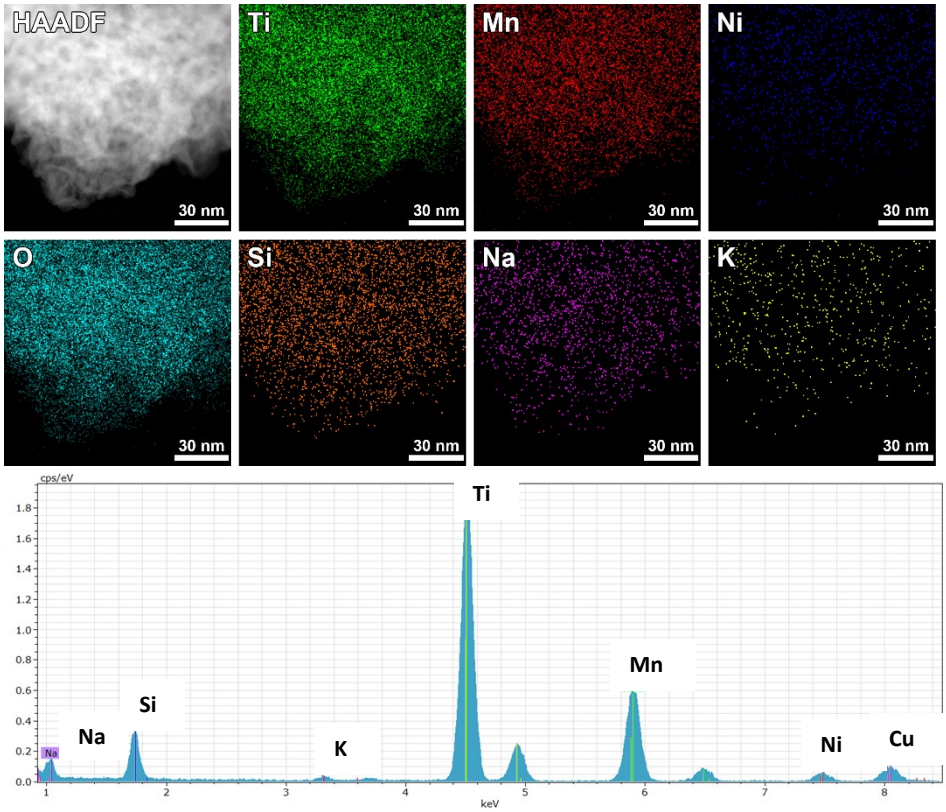

Figure S6. LNMO@LTO-200ºC: HAADF-STEM image, EDX maps and EDX spectra of amorphous matter. The atomic composition is Ti 62(2); Mn 21(1); Ni 2(1); Na 5(1); K 1(1); Si 9(3) (oxygen was not included in the calculation).

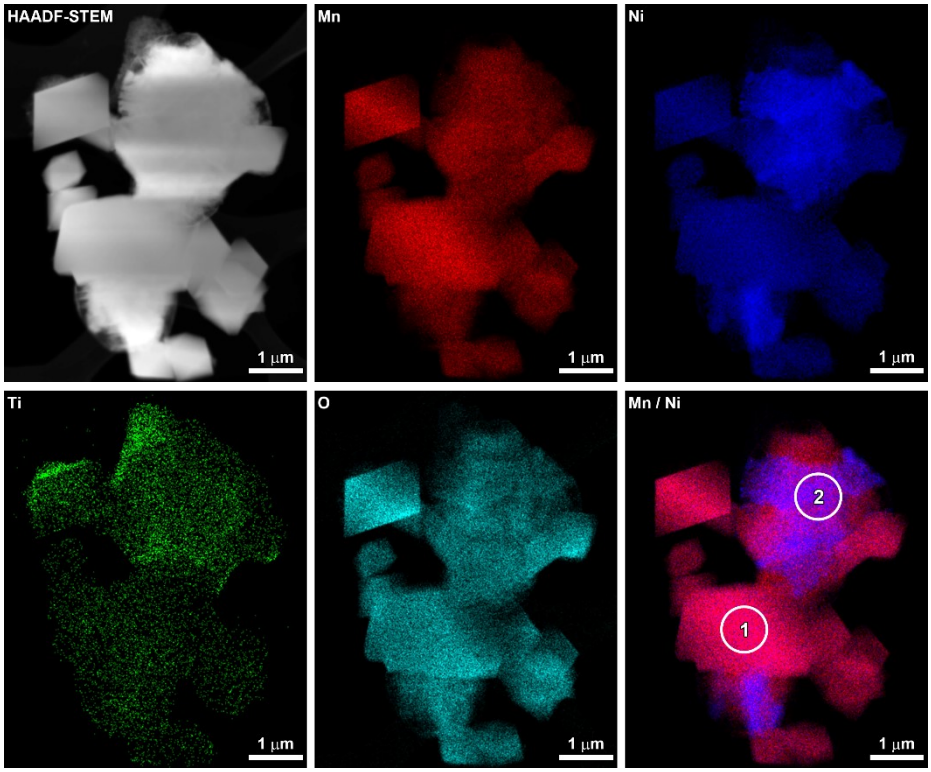

Figure S7. LNMO@LTO-500°C: HAADF-STEM image, individual STEM-EDX maps and Mn/Ni mixed map. The Ni and Mn content in the LNMO crystal when Li, Ti and O are neglected (area 1) is 23 and 77 at.% and in the Ni-rich area (area 2) is 52 and 48 at.%, respectively.

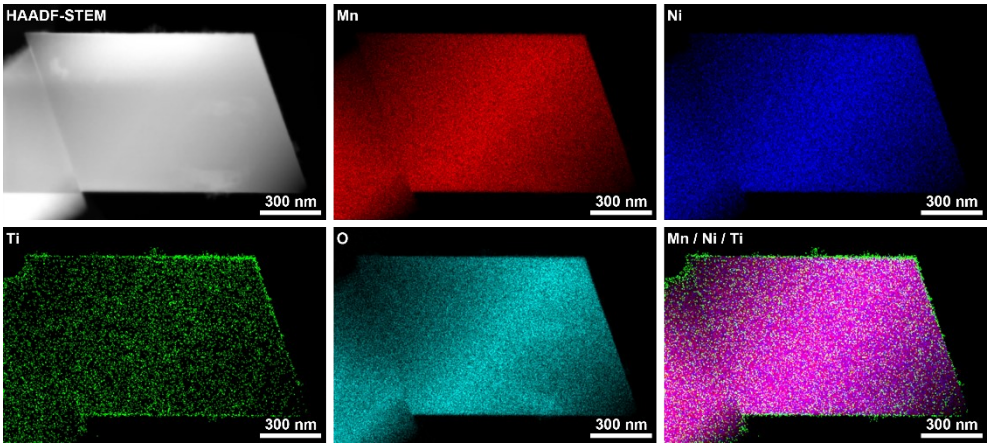

Figure S8. LNMO@LTO-500ºC: HAADF-STEM image, individual STEM-EDX maps and Mn/Ni/Ti mixed map. The crystal has uniform distribution of Ni and Mn with 23 and 77 at%, respectively when Li, Ti and O are neglected. Ti coating on the LNMO crystal is uniform and has a thickness about 2 nm.

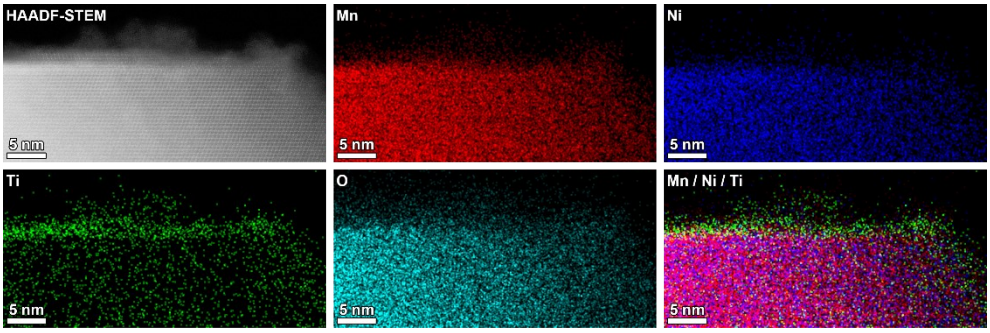

Figure S9. LNMO@LTO-500ºC: HAADF-STEM image, individual STEM-EDX maps and Mn/Ni/Ti mixed map of Ti-coated surface. The crystal is oriented along the [110] direction and both the core and the surface have a spinel structure exhibiting twinning near the surface. The

surface layer has Ti, Ni and Mn compositions of 24, 14 and 62 at. %, respectively, when Li and O are neglected.

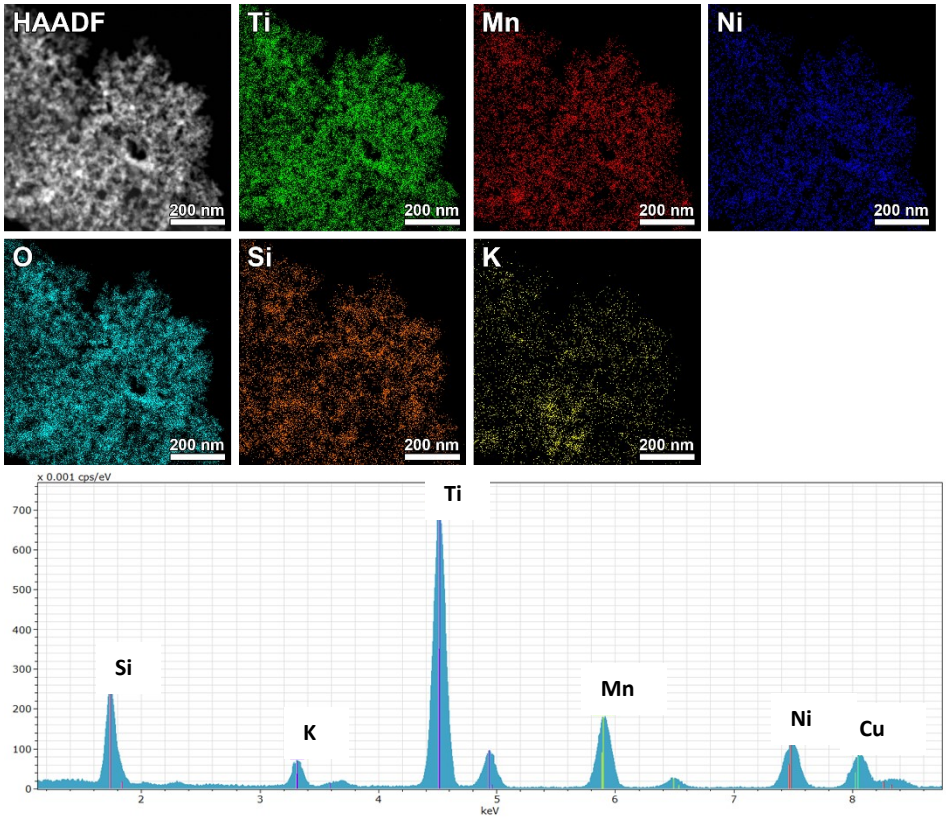

Figure S10. LNMO@LTO-500ºC: HAADF-STEM image, individual STEM-EDX maps and EDX spectra of rock salt nanoparticles. The atomic composition is Ti 52(3); Mn 14(1); Ni 11(2); K 5(2); Si 18(2) (oxygen was not included in the calculation).

Table S3. Electrical conductivity measurements of bare LNMO without (LNMO) or with (LNMO-500°C) 500°C anneal, amorphous LTO surface modified LNMO without (LNMO@LTO-200°C) or with (LNMO@LTO-500°C) 500°C anneal and LTO surface modification powder with 500°C anneal (LTO-500°C)

Powder	Electrical conductivity (σ) (S/cm)
LNMO	$3.1*10^{-7}$
LNMO@LTO-200°C	$2.7*10^{-7}$
LNMO-500°C	$5.0*10^{-7}$
LNMO@LTO-500°C	$2.8*10^{-7}$
LTO-500°C	$2.0*10^{-7}$

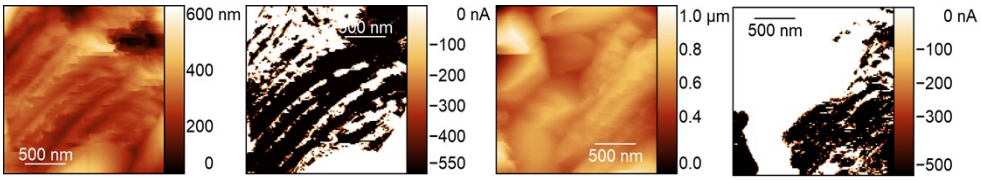

(a) (b) (c) (d)

Figure S11. C-AFM topography and current images for composite electrodes of (a,b) bare LNMO (LNMO-el.) and (c,d) amorphous LTO surface modified LNMO (LNMO@LTO-200°C-el.) (80/10/10 wt% AM/CB/PVDF). White areas in current images (b,d) are non-conductive, corresponding to 31.9 % in image (b) and 61.2% in image (d).

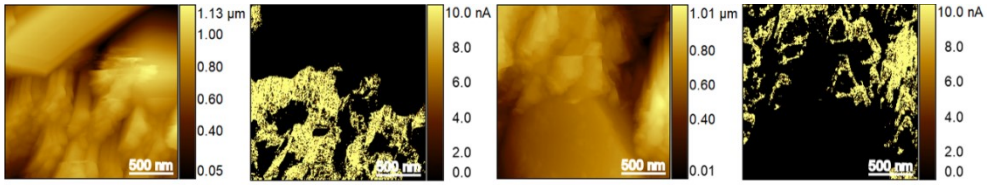

(a) (b) (c) (d)

Figure S12. C-AFM topography and current images for composite electrodes of (a,b) bare LNMO annealed at 500°C (LNMO-500°C-el.) and (c,d) amorphous LTO surface modified LNMO annealed at 500°C (LNMO@LTO-500°C-el.) composite electrodes (80/10/10 wt% AM/CB/PVDF). Black areas in current images (b,d) are non-conductive. Measured average current over the 2x2um area in (b) is 2.66 nA and in (d) is 1.87 nA.

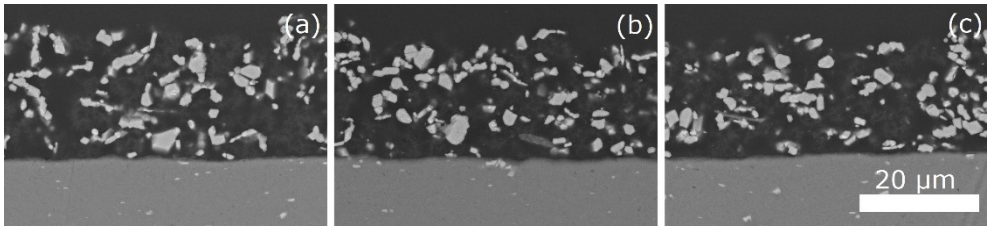

Figure S13. SEM cross-section images for fresh composite electrodes of (a) bare LNMO annealed at 500°C (LNMO-500°C-el.), (b) amorphous LTO surface modified LNMO (LNMO@LTO-200°C-el.) and (c) amorphous LTO surface modified LNMO annealed at 500°C (LNMO@LTO-500°C-el.)

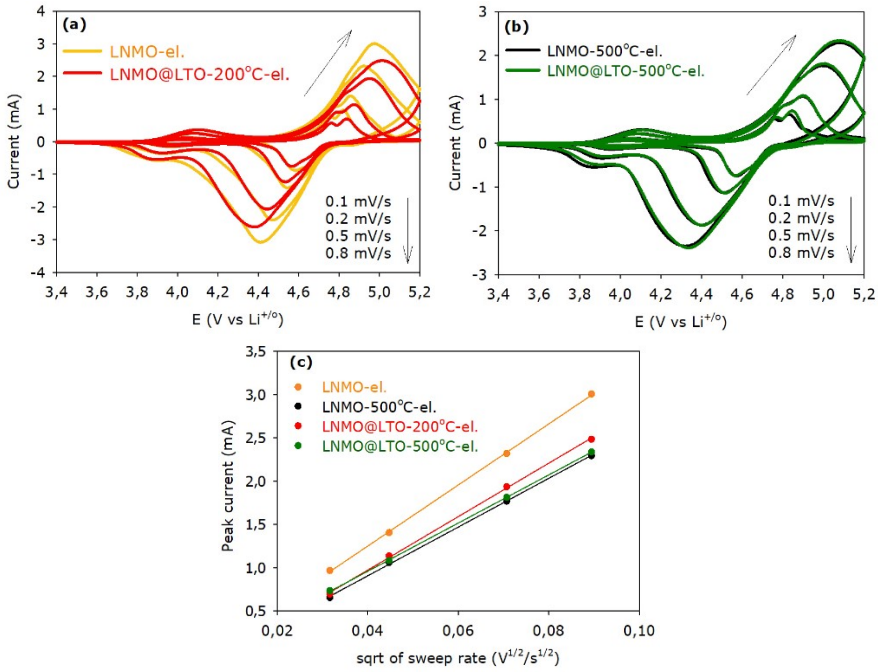

Figure S14. Cyclic voltammetries at increasing scan rates for electrodes of (a) bare LNMO (LNMO-el.) vs. amorphous LTO surface modified LNMO (LNMO@LTO-200°C-el.), (b) bare LNMO annealed at 500°C (LNMO-500°C-el.) vs. amorphous LTO surface modified LNMO annealed at 500°C (LNMO@LTO-500°C-el.) and (c) peak current vs. scan rate plots obtained from CVs in (a,b) for Ni^{3+} to Ni^{4+} oxidation reactions

Table S4. Lithium ion diffusion coefficients (D_{Li}) calculated for bare and surface modified LNMO powders. 'n' is the number of electrons involved in the reaction and C_{Li} is the Li^+ concentration in a unit cell

Sample	**Estimated formula***	**n (for Ni^{3+} →Ni^{4+})**	**slope**	**C_{Li} (mol/cm^3)**	**D_{Li} (cm^2/s)**
LNMO-el.	$Li^+ Ni^{2+}_{0.43} Mn^{3+}_{0.15} Mn^{4+}_{1.43} O^{2-}_4$	0.43	0.0353	0.0104	6.7*10^{-10}
LNMO@LTO -200^{o}C-el.	$Li^+ Ni^{2+}_{0.42} Mn^{3+}_{0.17} Mn^{4+}_{1.42} Ti^{4+}_x$	0.42	0.0309	0.0102	5.7*10^{-10}
LNMO-500^{o}C-el.	$Li^+ Ni^{2+}_{0.43} Mn^{3+}_{0.15} Mn^{4+}_{1.43} O^{2-}_4$	0.43	0.0281	0.0104	4.1*10^{-10}
LNMO@LTO -500^{o}C-el.	$Li^+ Ni^{2+}_{0.43} Mn^{3+}_{0.14} Mn^{4+}_{1.43} Ti^{4+}_x$	0.43	0.0278	0.0105	3.9*10^{-10}

**Based on capacity curve measurements at 0.05 C-rate*

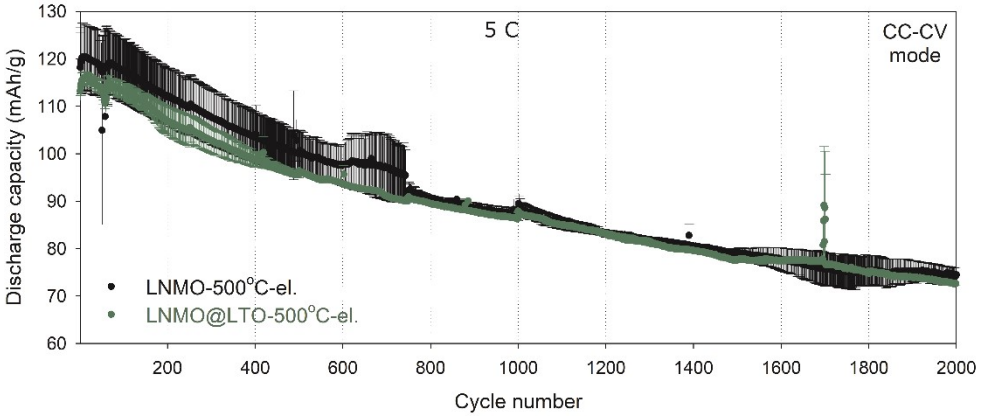

Figure S15. Cyclic stability measurements at 5 C rate in CC-CV mode at room temperature for electrodes of bare LNMO annealed at 500°C (LNMO-500°C-el.) and amorphous LTO surface modified LNMO annealed at 500°C (LNMO@LTO-500°C-el.). Data points show average of two or three measurements while error bars show the standard deviations.

Table S5. Summary of all the sample codes used to describe the powders and electrodes

Sample	**Type**	**Description**
LNMO	Powder	Bare $LiNi_{0.5}Mn_{1.5}O_{4-\delta}$
LNMO-500°C	Powder	Bare LNMO after 500°C anneal
LNMO@LTO-80°C	Powder	Amorphous LTO surface modified LNMO prec. gel
LNMO@LTO-200°C	Powder	Amorp. LTO surface modified LNMO
LNMO@LTO-500°C	Powder	Amorp. LTO surface modified LNMO after 500°C anneal

LTO-500^{o}C	Powder	LTO surface modification material
LNMO-el.	Electrode	Electrode made using the LNMO powder
LNMO-500^{o}C-el.	Electrode	Electrode made using the LNMO-500^{o}C powder
LNMO@LTO-200^{o}C-el.	Electrode	Electrode made using the LNMO@LTO-200^{o}C powder
LNMO@LTO-500^{o}C-el.	Electrode	Electrode made using the LNMO@LTO-500^{o}C powder

FTIR spectra of the bare and LTO surface modified LNMO powders without an anneal or with 500^{o}C annealing in dry air are shown in Figure S16. The absorption bands and their assignments are shown in Table S6. Absence of C=O stretching vibrations near 1720-1725 cm^{-1} for bare and LTO surface modified LNMO samples without, with a 200^{o}C or 500^{o}C anneal in dry air implies that the uncomplexed carboxylic acids have decomposed during the 200^{o}C and 500^{o}C thermal treatment steps.

$LiNi_{0.5}Mn_{1.5}O_4$ has disordered (Fd3m) and ordered ($P4_332$) crystalline forms with different degrees of Ni and Mn ordering. The 16d site is randomly occupied by Ni and Mn in disordered LNMO while Ni and Mn separately occupy the 4b and 12d sites, respectively, in the fully ordered type LNMO [2,3]. The 700 to 400 cm^{-1} regions of the FTIR spectra are enlarged for detailed examinations. A disordered (Fd3m) structure can be assigned to

LNMO since the number of observable peaks in 700 to 400 cm^{-1} region is only six while an ordered LNMO is known to have eight well-resolved peaks in the 700 to 400 cm^{-1} region [2]. The 480-460 cm^{-1} region is usually a double peak for the ordered LNMO powder, with another clear peak in the 420-430 cm^{-1} region. The 655 cm^{-1} absorption peak slightly loses intensity after the LTO surface modification, which might indicate slight increase in disordering during the surface modification process.

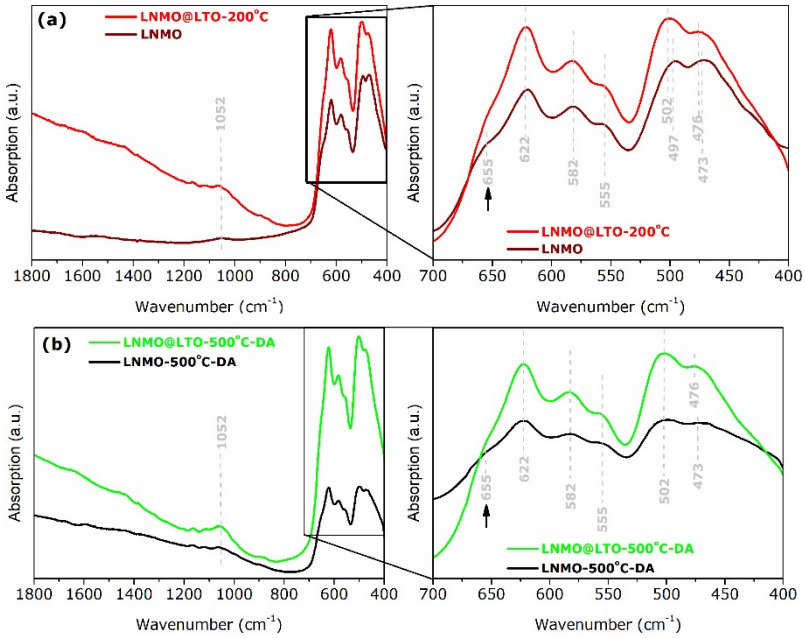

Figure S16. FTIR spectra of (a) bare LNMO ("LNMO") and amorphous LTO surface modified LNMO ("LNMO@LTO-200°C") powders, (b) bare LNMO powder annealed at 500°C in dry air flow ("LNMO-500°C-DA") and amorphous LTO surface modified LNMO powder annealed at 500°C in

dry air flow ("LNMO@LTO-500ºC-DA") (Blank KBr subtracted from all spectra)

Table S6. Absorption bands observed in FTIR spectra of bare and LTO surface modified LNMO powders and band assignments [2,4]

Wavenumber (cm^{-1})	**Vibrational assignment**
655	-
622	Mn-O A_{1g}
582	Ni-O F_{2g}
555	Mn-O A_{1g}
502, 497	Ni-O F_{2g}
476, 473	-

REFERENCES

1. Branford, W., Green, M.A. and Neumann, D.A. *Structure and ferromagnetism in Mn(4+) spinels: A $M_{0.5}Mn_{1.5}O_4$ (A = Li, Cu; M = Ni, Mg).* Chem. Mater., 2002. **14**: p. 1649-1656.

2. Kunduraci, M., et al., *Synthesis and Characterization of Nanostructured 4.7V $Li_xMn_{1.5}Ni_{0.5}O_4$ Spinels for High-Power Lithium-Ion Batteries.* Journal of The Electrochemical Society, 2006. **153**(7): p. A1345.

3. Duncan, H., et al., *Relationships between Mn3+Content, Structural Ordering, Phase Transformation, and Kinetic Properties in LiNixMn2–xO4Cathode Materials.* Chemistry of Materials, 2014. **26**(18): p. 5374-5382.

4. Ariyoshi, K., et al., *Topotactic Two-Phase Reactions of $LiNi_{1/2}Mn_{3/2}O_4$ ($P4_332$) in Nonaqueous Lithium Cells.* Journal of The Electrochemical Society, 2004. **151**(2): p. A296.